

---

# UNDERSTANDING THE DIFFICULTY OF LOW-PRECISION POST-TRAINING QUANTIZATION OF LARGE LANGUAGE MODELS

---

**Zifei Xu**  
d-Matrix  
Santa Clara, CA, USA  
xuzifei@d-matrix.ai

**Sayeh Sharify**  
d-Matrix  
Santa Clara, CA, USA  
sayehs@d-matrix.ai

**Wanzin Yazar**  
d-Matrix  
Santa Clara, CA, USA  
wyazar@d-matrix.ai

**Tristan Webb**  
d-Matrix  
Santa Clara, CA, USA  
twebb@d-matrix.ai

**Xin Wang**  
d-Matrix  
Santa Clara, CA, USA  
xwang@d-matrix.ai

October 21, 2024

## ABSTRACT

Large language models of high parameter counts are computationally expensive, yet can be made much more efficient by compressing their weights to very low numerical precision. This can be achieved either through post-training quantization by minimizing local, layer-wise quantization errors, or through quantization-aware fine-tuning by minimizing the global loss function. In this study, we discovered that, under the same data constraint, the former approach nearly always fared worse than the latter, a phenomenon particularly prominent when the numerical precision is very low. We further showed that this difficulty of post-training quantization arose from stark misalignment between optimization of the local and global objective functions. Our findings explains limited utility in minimization of local quantization error and the importance of direct quantization-aware fine-tuning, in the regime of large models at very low precision.

## 1 Introduction

Large language models (LLMs) have become remarkably powerful in recent years, and are increasingly deployed in real-world applications in practice [Xu et al., 2023, Wang et al., 2024, Zheng et al., 2023, Wu et al., 2023]. Despite their effectiveness, present-day LLMs are trained on modern GPUs, with its weights in floating point data type (typically `float16`). Thus, post-training compression techniques such as quantization, hold promise in making LLMs much more efficient at inference time, crucial for hardware acceleration [Yao et al., 2022, Kim et al., 2023a,b, Park et al., 2022, Frantar et al., 2022a, Lin et al., 2023].

Today, two distinct kinds of methods are popular to quantize an LLM’s weights while maintaining its generalization capabilities. One kind of techniques, namely *quantization-aware fine-tuning* (QAFT) optimizes a differentiable global objective just like at pretraining time, with quantization operations acting on the model weights; backpropagation and gradient updates are necessary in this case [Chee et al., 2024, Dettmers et al., 2023, 2024, Hu et al., 2021, Li et al., 2023, Huang et al., 2024]. The other type of methods seek to minimize layer-wise local errors that are due to the weight quantization; no backpropagation or gradient updates are necessary here [Frantar et al., 2022b, Xiao et al., 2023, Lee et al., 2024, Lin et al., 2023]. Note that both approaches require some, typically a small amount of, data to operate. In principle, at the limit where weight quantization error is small, minimizing the local losses should in turn minimize the global loss. Let us first introduce some formal notations before clarification of this point. Denote the LLM network by  $f_{\mathbf{W}} : \mathbb{D} \rightarrow \mathbb{R}^{|\mathcal{V}|}$ , which takes text input  $x \in \mathcal{D} \subset \mathbb{D}$  and generates logits  $f_{\mathbf{W}}(x)$  across vocabulary  $\mathcal{V}$ . Assume it is well-pretrained on language-modeling objective, *i.e.*  $\mathbf{W} = \arg \min_{\mathbf{W}'} \text{NLL}(x|f_{\mathbf{W}'})$  on a training data set  $\mathcal{D}$ . Here  $\mathbf{W} \triangleq (\mathbf{W}_1, \dots, \mathbf{W}_L)$  collects all layer-wise weights  $\mathbf{W}_l$  with  $l \in \{1, \dots, L\}$  indexing layers. In the following we

will also use vector notation  $\mathbf{w} \in \mathbb{R}^D$  to represent an equivalent, flattened version of  $\mathbf{W}$  in the  $D$ -dimensional weight space. Further denote by  $Q : \mathbb{R}^D \rightarrow \mathbb{R}^D$  the weight (fake-)quantization function (for procedural details see Section 3.2). We refer to the fake-quantized weights as *round-to-nearest* (RTN),  $\mathbf{W}_{\text{RTN}} \triangleq Q(\mathbf{W})$ .

QAFT methods essentially keep optimizing the global objective with quantization in the loop, *i.e.*

$$\mathbf{W}_{\text{QAFT}} = \arg \min_{\mathbf{W}'} \text{NLL}(\mathbf{x} | f_{Q(\mathbf{W}')}), \quad (1)$$

where  $\mathbf{x} \in \mathcal{D}$ ; due to the non-differentiability of  $Q(\cdot)$ , straight-through estimator is commonly used in gradient backpropagation.

In contrast, layer-wise quantization error minimization techniques seek to solve  $L$  distinct layer-wise optimization problems:

$$\mathbf{W}_l = \arg \min_{\mathbf{W}'_l} \text{MSE}(Q(\mathbf{W}'_l)\mathbf{x}_l, \mathbf{W}_l\mathbf{x}_l) \quad (2)$$

$$= \arg \min_{\mathbf{W}'_l} \|Q(\mathbf{W}'_l)\mathbf{x}_l - \mathbf{W}_l\mathbf{x}_l\|^2, \quad (3)$$

where  $\mathbf{x}_l$  is the input to the  $l$ -th layer when  $\mathbf{x} \in \mathcal{D}$  is passed through the network  $f$ . One popular method of this kind, namely GPTQ [Frantar et al., 2022a], derived from *optimal brain compression* (OBC) [Frantar and Alistarh, 2022], seeks to solve the layer-wise mean squared error (MSE) minimization problem by finding a less steeply rising direction in this local quadratic loss landscape, through efficient computation of the Hessian of the local MSE losses. We denote a GPTQ-optimized network’s weights by  $\mathbf{W}_{\text{GPTQ}}$ .

Intuitively, minimization of the local MSE losses as described above *should* have similar effects as minimizing the global NLL loss, because at the limit where local MSEs are close to 0, the global NLL ( $\mathbf{x} \in \mathcal{D}_{\text{test}} | f_{\mathbf{W}_{\text{GPTQ}}}$ ) should be close to NLL ( $\mathbf{x} \in \mathcal{D}_{\text{test}} | f_{\mathbf{W}}$ ), the full-precision pre-trained model. But is this true in practice when local MSEs are not necessarily close to zero?

In this work, by conducting a systematic study on a number of LLMs, we observed and reported a surprising misalignment between the aforementioned two quantization approaches. Specifically, we showed that optimization of the local MSE losses often could lead to substantially suboptimal global NLL loss, and a direct minimization of the global NLL does not necessarily lead to lower local MSE losses, especially when the quantization precision was very low.

Further, through loss-landscape mapping, we offered an explanation of why the post-training quantization by local loss minimization suffered from the difficulty in producing well-generalizing quantized networks at low numerical precision.

We believe our work would inform future LLM quantization practices.

## 2 Related work

**Post-training quantization** Quantization reduces the memory and computational demands of neural networks by converting either their weights or activations from full precision to lower precision formats, like 8-bit integers. Post-training quantization (PTQ) techniques achieve this by representing weights and/or activations with smaller precisions without partially or fully retraining the network. Several PTQ techniques have emerged to reduce deployment cost of LLMs, using different approaches to quantize the models. Some methods focus on identifying outlier features that are difficult to quantize and either represent them with a higher precision, *e.g.* LLM.int8() [Dettmers et al., 2022], or mitigate their quantization error by adding additional operations to the network, such as SmoothQuant [Xiao et al., 2023], AWQ [Lin et al., 2023], and OWQ [Lee et al., 2024].

Other PTQ methods employ adaptive rounding techniques to compensate for quantization errors. For instance, OBC [Frantar and Alistarh, 2022] quantizes weights one-by-one in a specific order based on the approximate second-order information of the weights, and adjusts the remaining weights to compensate for the quantization error. GPTQ [Frantar et al., 2022a], also known as OPTQ [Frantar et al., 2022b], extends OBC by enabling parallel quantization of weight matrices, applying the same quantization order to all rows of the weight matrix. Similarly, QuIP [Chee et al., 2024] uses an adaptive rounding procedure to minimize a quadratic proxy objective of the quantization error.

**Quantization-aware fine-tuning** Fine-tuning LLMs adapts them to specific tasks, ensuring that they generate accurate and contextually relevant outputs. However, the expensive parameter updates during fine-tuning have drawn significant attention to optimizing its efficiency. Parameter efficient fine-tuning (PEFT) involves reusing some of the pretrained model’s parameters and selectively fine-tuning a subset of parameters for the downstream tasks. Some of PEFT methods are: LoRA [Hu et al., 2021], QLoRA [Dettmers et al., 2024], L4Q [Jeon et al., 2024], LoftQ [Li et al., 2023], Prefix and

Prompt Tuning [Li and Liang, 2021, Lester et al., 2021, Qin and Eisner, 2021, Liu et al., 2023], IA3 [Liu et al., 2022], and PEQA [Kim et al., 2024].

LoRA, QLoRA, L4Q, and LoftQ freeze pretrained model parameters and insert task-specific parameters between the frozen layers. These new parameters undergo fine-tuning. Extending this adapter-based approach, the abovementioned methods employ rank decomposition to significantly reduce the number of trainable parameters during fine-tuning [Hu et al., 2021, Dettmers et al., 2024, Jeon et al., 2024, Li et al., 2023]. In prefix and prompt tuning, the parameters of an original large language model are frozen, and only the trainable prompt embeddings are fine-tuned [Li and Liang, 2021, Lester et al., 2021, Qin and Eisner, 2021, Liu et al., 2023]. Similarly, in IA3 only the hidden state parameters are fine-tuned [Liu et al., 2022].

PEQA is a memory-efficient fine-tuning method for quantized LLMs that updates only the quantization scale, keeping the integer matrix frozen [Kim et al., 2024].

**Ultra-low precision pretraining** There has been recent efforts to binarize LLMs by quantizing them to ultra-low bit-widths. For instance, PB-LLM [Shang et al., 2023] and SpQR [Dettmers et al., 2023] employ a mixed-precision quantization technique, representing the majority of the weights with a single bit and retaining a small portion of the weight in the original high precision or `int8`. BiLLM [Huang et al., 2024] utilize Hessian information to identify salient weights, and non-salient weights. It minimizes the compression loss through an effective binary residual approximation of salient weights and grouped quantization of non-salient weights. BitNet [Wang et al., 2023], on the other hand, replaces the linear layers in the transformer architecture by a binary linear layer with only two weight values, maintaining other components in high-precision. BitNet b1.58 [Ma et al., 2024] is an extension of BitNet that utilizes ternary quantization for its weights. BitNet b1.58 achieves better accuracy in downstream tasks compared to BitNet.

**Loss landscape analysis** Analysis of deep neural networks’ loss landscape has long been a tool toward understanding of the generalization properties of the optimized model [Li et al., 2018, Ghorbani et al., 2019, Sagun et al., 2017, 2018], as well as in explaining difficulties arising in efficient network optimization processes [Evcı et al., 2020].

## 3 Methods

### 3.1 Models and data set

We experimented with 11 models from 3 model families, namely GPT-2 [Radford et al., 2019], OPT [Zhang et al., 2022] and Llama 2 [Touvron et al., 2023]. All models were served by the Hugging Face Model Hub <sup>1</sup>.

We used the WikiText-2 [Merity et al., 2016] data set in all experiments. Unless noted otherwise, the training split used in all procedures was of 128 examples, each of the maximum sequence length supported by the model being experimented. For test and validation, the entire split was used.

### 3.2 Numerical data types and quantizer calibration

We experimented with 5 integer data types for weight quantization, namely `int8`, `int6`, `int4`, `int3` and `int2`, of varied numerical precision. For integer with  $B$ -bit precision, encoding range is symmetric, *i.e.*  $\{-2^{B-1} + 1, \dots, 2^{B-1} - 1\}$ , excluding  $-2^{B-1}$ ; for example, `int2` quantization is effectively ternary,  $\{-1, 0, 1\}$ .

We used PyTorch’s quantization API <sup>2</sup> to obtain the weight fake-quantization functions  $Q(\cdot)$ . The quantization scheme used was per-tensor symmetric <sup>3</sup>. The scaling factor  $a_l$ ’s of the fake-quantizer was determined by mean squared quantization error minimization, *i.e.*  $a_l = \arg \min_a \|Q_a(\mathbf{W}_l) - \mathbf{W}_l\|^2, \forall l \in \{1, \dots, L\}$ , by means of PyTorch’s `HistogramObserver` mechanism. For simplicity, only weights of layers in the transformer stack were quantized, sparing other weights such as those in embedding and prediction head layers.

### 3.3 GPTQ

We followed the original GPTQ procedure [Frantar et al., 2022a] exactly except for one change described below. As reported by other adopters of GPTQ, *e.g.* <https://huggingface.co/TheBloke>, different choices of the dampening factor as a hyperparameter in the GPTQ procedure could lead to outcomes of varied qualities. In order to eliminate

<sup>1</sup>All models were accessed from official repositories hosted by <https://huggingface.co/> in April 2024.

<sup>2</sup>See <https://pytorch.org/docs/stable/quantization.html>.

<sup>3</sup>Note that different quantization schemes and/or different data types of the same precision often result in different generalization quality of the quantized network, determined by the granularity of a channel/group/block-wise scheme. Here we choose to use the simplest scheme in order to conduct a controlled scientific study with fewest confounding factors.

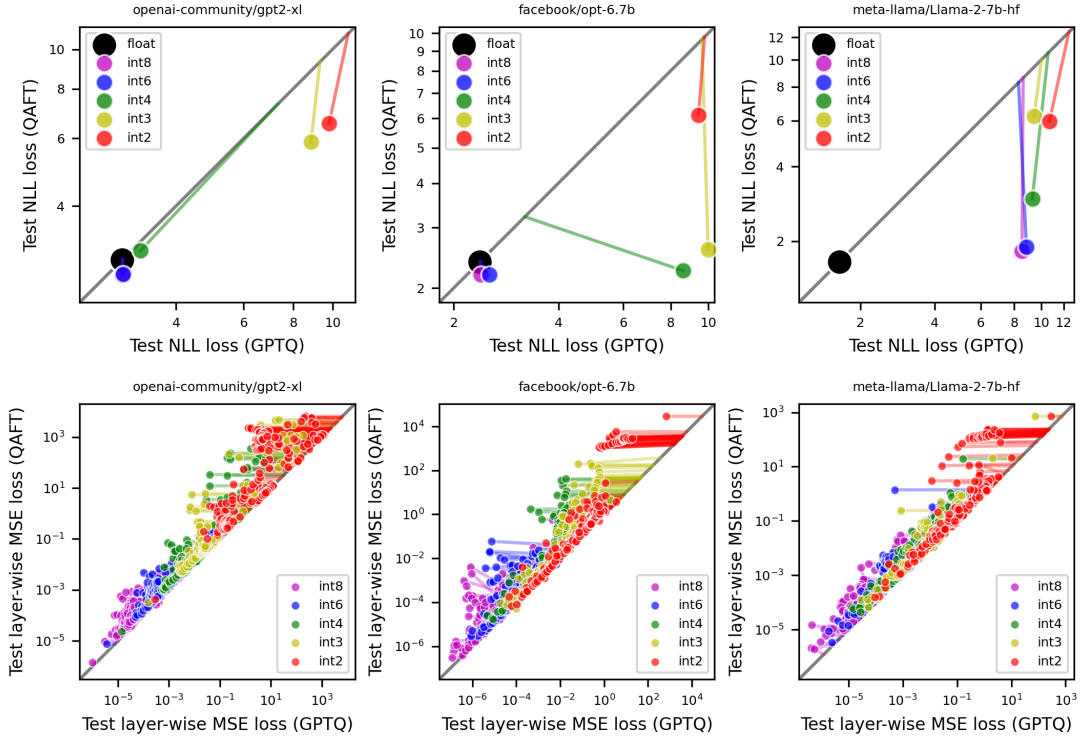


Figure 1: **A misalignment between minimization of the global NLL loss (by QAFT) and minimization of the local layer-wise MSE losses (by GPTQ).** Each panel plots results for a single model and for a certain type of loss metric. Panels in the upper row show results of global NLL loss, whereas those in the lower row of layer-wise local MSE losses. The three columns correspond to three models whose names are labeled at the top of each panel. All data are plotted for direct comparison between QAFT (vertical axis) and GPTQ (horizontal axis), with the gray diagonal line marking identity. If present, the block dot represents data of the full-precision floating point model. The colored dots chart losses after QAFT and GPTQ, from each of which a colored line emanates and intersects the diagonal, marking the loss of the RTN-quantized model. Each symbol in plots of the lower row represents an individual layer whose weight matrix was subject to quantization.

this confounding factor, we performed hyperparameter tuning for the GPTQ dampening factor over a search space of  $\{10^{-3}, \dots, 10^4\}$ , in a layer-wise manner. As mentioned above, 128 examples from the training split were used for the GPTQ procedure, consistent with the original work [Frantar et al., 2022a].

### 3.4 Quantization-aware fine-tuning (QAFT)

To perform QAFT, the exact same 128 training examples were used as above, for a fair comparison. We ran QAFT for 8 epochs, *i.e.* in total 1024 training iterations (see Appendix B for effect of iterations). Straight through estimator (STE) [Hinton et al., 2012, Bengio et al., 2013] was employed in backpropagation through quantization functions. Only quantized weights in the transformer network were subject to gradient updates. We used the AdamW optimizer [Loshchilov and Hutter, 2017] without weight decay, and with a linear learning rate decay schedule of 1 order of magnitude. We ran a hyperparameter grid search over 4 initial learning rate values,  $\{10^{-6}, 10^{-5}, 10^{-4}, 10^{-3}\}$  for all models except for Llama-2-7b-hf, in which case it was  $\{10^{-6}, 10^{-3}\}$  (see Appendix A for more details on hyperparameter tuning); best NLL loss over the validation split was chosen.

## 4 Results

### 4.1 GPTQ vs. QAFT under the same data constraint

First, we asked whether minimization of the local MSE losses through GPTQ aligned with minimization of the global NLL loss through QAFT. In order to answer this question, we conducted the GPTQ and QAFT procedures as described

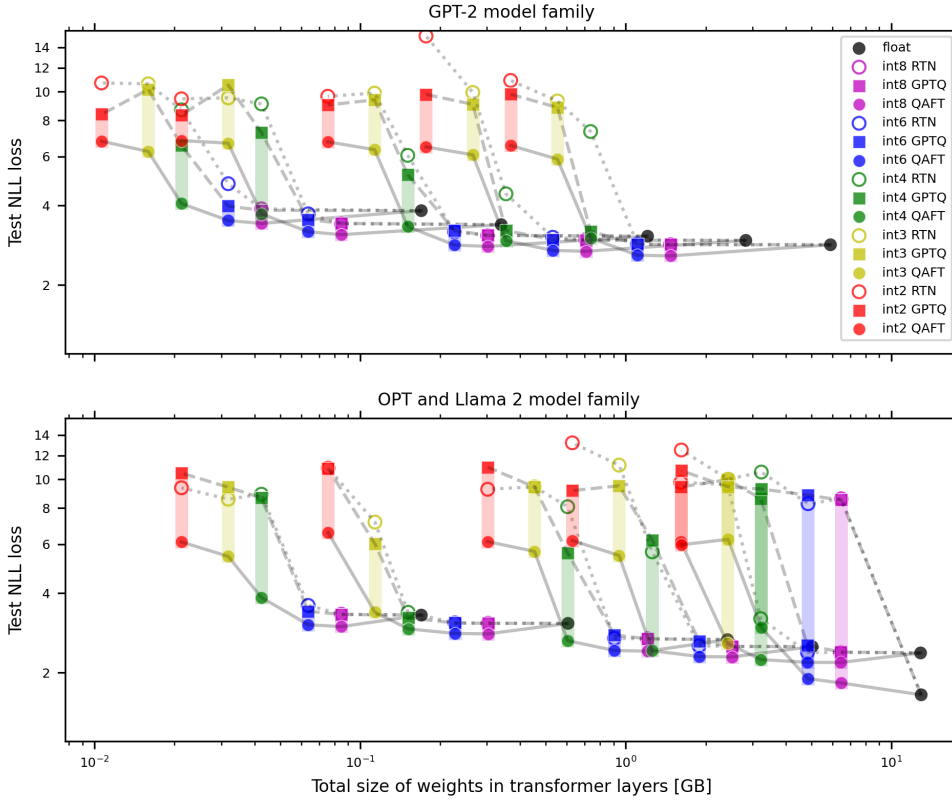


Figure 2: **Tradeoff between quantized model generalization and its weight size.** **Upper:** models from the GPT-2 model family: `distilgpt2`, `gpt2`, `gpt2-medium`, `gpt2-large` and `gpt2-xl`. **Lower:** models from the OPT and Llama 2 families: `opt-250m`, `opt-350m`, `opt-1.3b`, `opt-2.7b`, `opt-6.7b` and `Llama-2-7b-hf`. Black circles represent the full-precision models. Hollow colored circles are RTN-quantized models, solid colored circles QAFT-quantized models, and solid colored squares GPTQ-quantized models. Dotted, dashed and solid gray lines connect quantized solutions from the same model produced by RTN, GPTQ and QAFT, respectively. We highlight the difference between GPTQ- and QAFT-quantized models with colored, transparent, vertical strips, for each quantized model.

in Section 3 on all experimented LLMs. We reported, for each quantized networks produced by both methods, the global NLL loss and local layer-wise MSE losses evaluated on the test data set.

In Figure 1, we plotted the global NLL and local MSE losses for `gpt2-xl`, `opt-6.7b` and `llama2-7b`, three example LLMs that were the largest among each model family we experimented with. As evident in the upper row of plots showing global NLL losses, the colored dots were always below the diagonal identity line, indicating that NLL loss after QAFT was always lower than that after GPTQ for the same model at a particular precision. At certain precision, sometimes performing GPTQ led to NLL losses even higher than that of RTN. In contrast, the lower row of plots illustrating layer-wise local MSE losses showed a remarkably different story. GPTQ always lowered layer-wise MSE losses, precisely as it was designed to do, but QAFT hardly ever reduced layer-wise MSEs from the RTN level and in most cases increased the layer-wise MSE losses.

These results suggested that direct minimization of the global NLL loss did not necessarily lead to a reduction of layer-wise local MSEs. Likewise, indirect minimization of layer-wise MSEs also did not guarantee that the global NLL loss would decrease, particularly for `int2` quantization of most experimented models. Since the generalization capability of a quantized model is measured by the global NLL loss, minimizing layer-wise MSEs did not seem an ideal surrogate objective function to optimize, in light of the observed misalignment. This effect was especially prominent in the case of low precision formats, where QAFT was remarkably more effective than GPTQ; in Appendix B, we showed that just very few iterations of gradient updates with QAFT could achieve a much better generalizing quantized model than GPTQ.

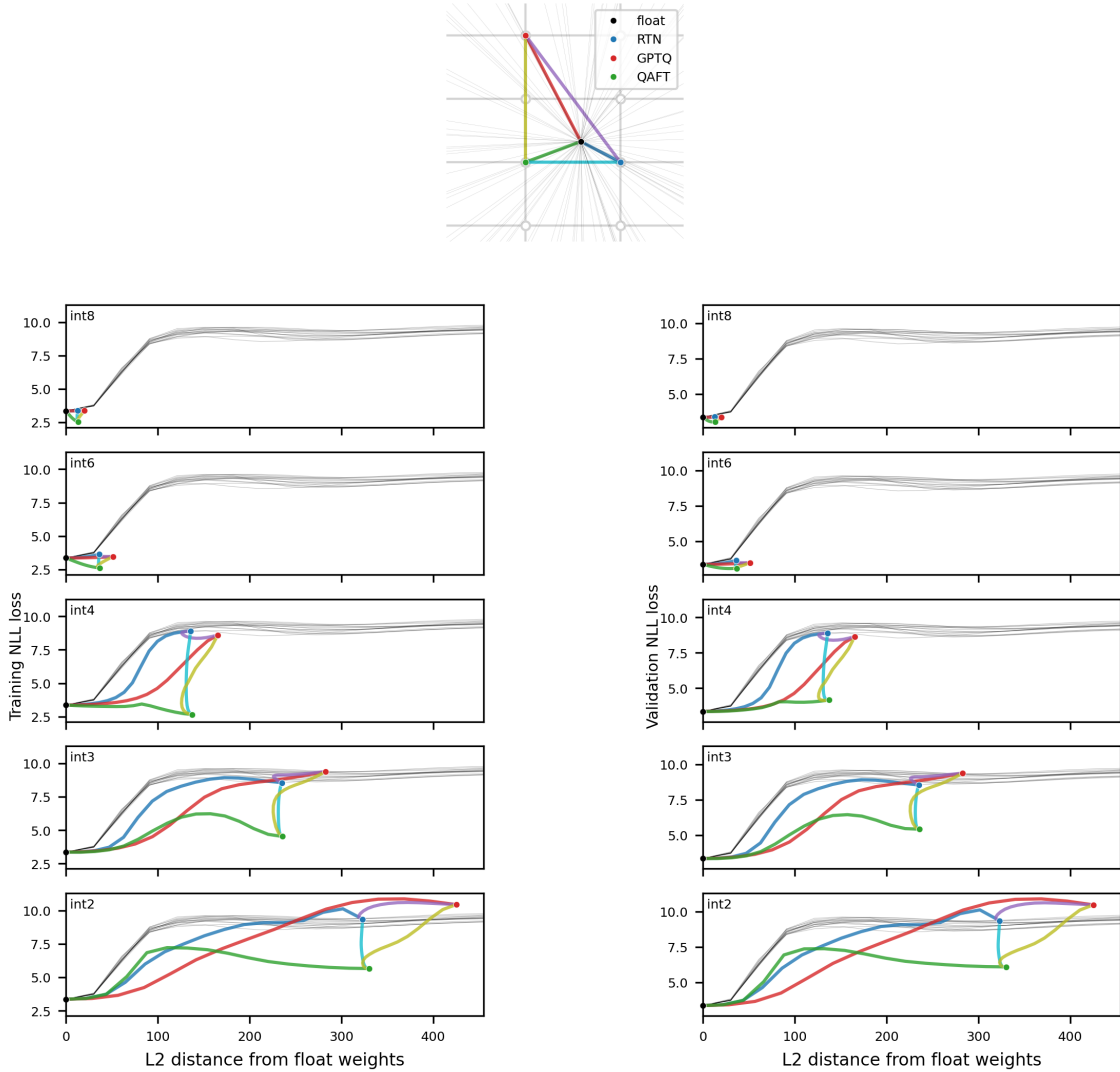


Figure 3: **Loss landscape analysis of quantized model weights.** Data illustrated here are from opt-125m, a network small enough for numerous loss evaluations in order to map the loss landscape in the neighborhood around pretraining convergence. In the legend at the top, we illustrate the mapping strategy in a 2-dimensional cartoon, which captures key concepts in the  $D$ -dimensional weight space. The black dot in the middle marks the pretraining convergence  $w$ . The continuous loss landscape is probed first by measuring loss at  $w + \lambda \hat{e}$ , *i.e.* pretrained weight subject to random perturbation  $\hat{e} \sim \mathcal{S}^D$  sampled uniformly from the  $D$ -dimensional unit sphere. We sweep  $\lambda \in \mathbb{R}^+$  (thin, light gray lines emanating from the black circle) to map the radial loss landscape along a specific random direction  $\hat{e}$ . The gray grid represents the representable weight values prescribed by the weight quantizer  $Q(\cdot)$ , out of which we show three key quantized weights under question:  $w_{\text{RTN}} = Q(w)$  (blue circle),  $w_{\text{QAFT}}$  (green circle), and  $w_{\text{GPTQ}}$  (red circle). We measure the loss function at these key points as well as those along the linear segment resulting from a convex combination of two of these (colored lines). We plot the radial loss landscape (NLL loss against  $\ell_2$  distance from  $w$ ) in the lower panels, training loss on the left and validation loss on the right. Graphical symbols of points and segments are consistent with the legend at the top.

## 4.2 Scaling with LLM size and numerical precision

Next, we questioned how the generalization abilities of quantized models produced by RTN, QAFT and GPTQ, scaled as a function of model size and numerical precision. In order to gain a comprehensive understanding of the matter, we aggregated all models in a single tradeoff graph of test NLL loss plotted against total transformer weight sizes in gigabytes (Figure 2).

As shown in Figure 2, the Pareto front was dominantly occupied by networks quantized through QAFT. In the top panel for the GPT-2 model family, the Pareto front mainly consisted of solutions by QAFT with `int6` and `int8`. At a same model size, a GPT-2 model quantized to `int6` and `int8` outperformed both a full-precision counterpart with fewer parameters, and one quantized to lower precision with more parameters. We observed a similar pattern with models from the OPT and Llama 2 families, as shown in the lower panel of Figure 2. Here, `int4`, `int6` and `int8` models produced by QAFT dominated the Pareto front.

In both panels of Figure 2, we highlighted the difference in test NLL between QAFT and GPTQ solutions, by the colored, transparent and vertical strips. Evidently, models quantized by QAFT was better generalizing at lower precision, such as `int2`, `int3` and `int4`. This observation was consistent with the misalignment between the global NLL loss and the layer-wise local MSE losses was more prominent at low numerical precision.

## 4.3 Explanation of the misalignment from a loss landscape perspective

Finally, we asked why minimization of local layer-wise MSE losses did not align with minimizing the global NLL loss, especially in case of quantization to low numerical precision. To answer this question, we resorted to mapping of the global NLL loss landscape in the  $D$ -dimensional weight space in the neighborhood of the pretrained weights  $\mathbf{w} \in \mathbb{R}^D$ .

We presented an example in Figure 3 of `opt-125m`, a model small enough for numerous loss evaluations.

First, we measured NLL loss along a number of random directions emanating from  $\mathbf{w}$  (the thin, light gray lines in Figure 3). It was evident from the radial mapping that  $\mathbf{w}$  sat near the bottom of an attractive basin. The near-convergence neighborhood looked like quadratic, and the loss profiles along randomly sampled directions were rather similar to each other. This is consistent with prior analysis of the loss Hessian spectra showing the presence of a large bulk subspace and a small number of outliers [Sagun et al., 2017, 2018, Ghorbani et al., 2019]; thusly, a random linear combination of Hessian eigenvectors would, with high probability, stay within the bulk subspace, making independent radial loss profile look very similar to each other. Beyond the near-convergence locality, notably, the radial loss landscape quickly deviated from a good second-order approximation and plateaued at a high level, demarcating an  $\ell_2$  neighborhood size  $R(\mathbf{w})$  that defined the attractive basin.

Next, we charted the loss landscape of the quantized weights via RTN, QAFT and GPTQ, and of linear interpolation segments between them (colored circles and line segments in the Figure 3). We made the following observations.

- $\mathbf{w}_{\text{RTN}}$  (blue circle), the quantized weight nearest to  $\mathbf{w}$ , was within the attractive basin for `int8` and `int6`, clearly outside of it for `int3` and `int2`, and around the border for `int4`.
- $\mathbf{w}_{\text{GPTQ}}$  (red circle), was significantly more distant from  $\mathbf{w}$  than  $\mathbf{w}_{\text{RTN}}$ , but the direction from  $\mathbf{w}$  leading to  $\mathbf{w}_{\text{GPTQ}}$  (red segment) was much less steep than any typical directions. The loss values at  $\mathbf{w}_{\text{GPTQ}}$  were low for `int8` and `int6`, and high for `int4`, `int3` and `int2`, not much different from those at  $\mathbf{w}_{\text{RTN}}$  for the same precision.
- $\mathbf{w}_{\text{QAFT}}$  (green circle), was not materially more distant from  $\mathbf{w}$  than  $\mathbf{w}_{\text{RTN}}$ , but at a significantly lower loss level.
- Notably, all quantized weights more distant from  $\mathbf{w}$  than the radius of the attractive basin, did not seem to be simply connected with  $\mathbf{w}$ . By *simply connected*, we meant that the loss profile along the linear segment connecting the two is monotonic without a ridge in the middle.

Based on these observations of the analysed loss landscape, we were able to explain the experimental findings reported in previous sections. The minimization of layer-wise local MSE by GPTQ, as expected, was successful in picking a much less steeply rising direction emanating from  $\mathbf{w}$ , along which, if the quantized  $\mathbf{w}_{\text{GPTQ}}$  was not distant, stayed at a lower loss level, as in the cases for `int8` and `int6`; but if the quantized  $\mathbf{w}_{\text{GPTQ}}$  was substantially distant from  $\mathbf{w}$ , as in the cases for `int3` and `int2`, the initial shallow rise near  $\mathbf{w}$  no longer mattered, resulting in very high loss values at the eventual  $\mathbf{w}_{\text{GPTQ}}$  instead. In contrast, even at localities distant from  $\mathbf{w}$ , QAFT still made material progress from  $\mathbf{w}_{\text{RTN}}$ , leading to  $\mathbf{w}_{\text{QAFT}}$  with significantly lower loss, albeit no longer simply connected to  $\mathbf{w}$ , likely in another distinct attractive basin, reminiscent of similar observations in training of sparse neural networks [Evci et al., 2020].

Our results suggested that, the relative relationship between the sizes of the attractive basin near convergence  $R(\mathbf{w})$ , and of the weight perturbation due to quantization  $\|\Delta\mathbf{w}\| = \|\mathbf{w}_{\text{RTN}} - \mathbf{w}\|$ , seemed to predict how much minimizing local losses and minimizing the global loss would align with each other. When the latter was substantially larger than the former, misalignment invariably occurred.

## 5 Discussion

In this work, we conducted a systematic study contrasting and comparing the effectiveness of post-training quantization method GPTQ and quantization-aware fine-tuning (QAFT); the former minimized layer-wise local quantization errors whereas the latter minimized the global training loss. We discovered that, with our experimental setting under the same low training data constraint (128 training examples), GPTQ was not as effective as QAFT in nearly all cases. Additional experiments showed that, in certain cases, just a few QAFT iterations could overtake GPTQ in producing a better generalizing LLM (see Appendix B).

We found, rather surprisingly, that in the cases where GPTQ fared significantly worse than QAFT, the minimization of the local MSE and the global NLL losses did not necessarily align with each other. We further elucidated, through loss landscape analysis, that such misalignment was a characteristic behavior when the weight perturbation due to quantization was significantly larger than the radius of the attractive basin at the pretraining convergence, a frequent situation consequent from very low precision weight quantization.

Our study demonstrated an apparent lack of correlation between the generalization capabilities of a quantized neural network and the local quantization errors in its component layers, the latter of which often used as a metric to evaluate the quality of quantization schemes. We call for caution on generalization of the utility of local error minimization-based post-training quantization techniques in practice, and provided a new perspective toward understanding the difficulty and identification of the circumstances under which applying these methods were effective.



## References

- Yoshua Bengio, Nicholas Léonard, and Aaron Courville. Estimating or propagating gradients through stochastic neurons for conditional computation. *arXiv preprint arXiv:1308.3432*, 2013.
- Jerry Chee, Yaohui Cai, Volodymyr Kuleshov, and Christopher M De Sa. QuIP: 2-bit quantization of large language models with guarantees. *Advances in Neural Information Processing Systems*, 36, 2024.
- Tim Dettmers, Mike Lewis, Younes Belkada, and Luke Zettlemoyer. LLM.int8(): 8-bit matrix multiplication for transformers at scale, 2022. *CoRR abs/2208.07339*, 2022.
- Tim Dettmers, Ruslan Svirschevski, Vage Egiazarian, Denis Kuznedelev, Elias Frantar, Saleh Ashkboos, Alexander Borzunov, Torsten Hoefler, and Dan Alistarh. SpQR: A sparse-quantized representation for near-lossless llm weight compression. *arXiv preprint arXiv:2306.03078*, 2023.
- Tim Dettmers, Artidoro Pagnoni, Ari Holtzman, and Luke Zettlemoyer. QLoRA: Efficient finetuning of quantized llms. *Advances in Neural Information Processing Systems*, 36, 2024.
- Utku Evci, Fabian Pedregosa, Aidan Gomez, and Erich Elsen. The difficulty of training sparse neural networks. 2020.
- Elias Frantar and Dan Alistarh. Optimal brain compression: A framework for accurate post-training quantization and pruning. *Advances in Neural Information Processing Systems*, 35:4475–4488, 2022.
- Elias Frantar, Saleh Ashkboos, Torsten Hoefler, and Dan Alistarh. GPTQ accurate post-training quantization for generative pre-trained transformers. *arXiv preprint arXiv:2210.17323*, 2022a.
- Elias Frantar, Saleh Ashkboos, Torsten Hoefler, and Dan Alistarh. OPTQ: Accurate quantization for generative pre-trained transformers. In *The Eleventh International Conference on Learning Representations*, 2022b.
- Behrooz Ghorbani, Shankar Krishnan, and Ying Xiao. An investigation into neural net optimization via hessian eigenvalue density. 2019.
- Geoffrey Hinton, Li Deng, Dong Yu, George E Dahl, Abdel-rahman Mohamed, Navdeep Jaitly, Andrew Senior, Vincent Vanhoucke, Patrick Nguyen, Tara N Sainath, et al. Deep neural networks for acoustic modeling in speech recognition: The shared views of four research groups. *IEEE Signal processing magazine*, 29(6):82–97, 2012.
- Edward J Hu, Yelong Shen, Phillip Wallis, Zeyuan Allen-Zhu, Yuanzhi Li, Shean Wang, Lu Wang, and Weizhu Chen. LoRA: Low-rank adaptation of large language models. *arXiv preprint arXiv:2106.09685*, 2021.
- Wei Huang, Yangdong Liu, Haotong Qin, Ying Li, Shiming Zhang, Xianglong Liu, Michele Magno, and Xiaojuan Qi. BiLLM: Pushing the limit of post-training quantization for llms. *arXiv preprint arXiv:2402.04291*, 2024.
- Hyesung Jeon, Yulhwa Kim, and Jae-joon Kim. L4Q: Parameter efficient quantization-aware training on large language models via lora-wise lsq. *arXiv preprint arXiv:2402.04902*, 2024.
- Jeonghoon Kim, Jung Hyun Lee, Sungdong Kim, Joonsuk Park, Kang Min Yoo, Se Jung Kwon, and Dongsoo Lee. Memory-efficient fine-tuning of compressed large language models via sub-4-bit integer quantization. *Advances in Neural Information Processing Systems*, 36, 2024.
- Sehoon Kim, Coleman Hooper, Amir Gholami, Zhen Dong, Xiuyu Li, Sheng Shen, Michael W Mahoney, and Kurt Keutzer. Squeezellm: Dense-and-sparse quantization. *arXiv preprint arXiv:2306.07629*, 2023a.
- Young Jin Kim, Rawn Henry, Raffy Fahim, and Hany Hassan Awadalla. Finequant: Unlocking efficiency with fine-grained weight-only quantization for llms. *arXiv preprint arXiv:2308.09723*, 2023b.
- Changhun Lee, Jungyu Jin, Taesu Kim, Hyungjun Kim, and Eunhyeok Park. OWQ: Outlier-aware weight quantization for efficient fine-tuning and inference of large language models. In *Proceedings of the AAAI Conference on Artificial Intelligence*, volume 38, pages 13355–13364, 2024.
- Brian Lester, Rami Al-Rfou, and Noah Constant. The power of scale for parameter-efficient prompt tuning. *arXiv preprint arXiv:2104.08691*, 2021.
- Hao Li, Zheng Xu, Gavin Taylor, Christoph Studer, and Tom Goldstein. Visualizing the loss landscape of neural nets. 2018.
- Xiang Lisa Li and Percy Liang. Prefix-tuning: Optimizing continuous prompts for generation. *arXiv preprint arXiv:2101.00190*, 2021.
- Yixiao Li, Yifan Yu, Chen Liang, Pengcheng He, Nikos Karampatziakis, Weizhu Chen, and Tuo Zhao. LoftQ: Lora-fine-tuning-aware quantization for large language models. *arXiv preprint arXiv:2310.08659*, 2023.
- Ji Lin, Jiaming Tang, Haotian Tang, Shang Yang, Xingyu Dang, and Song Han. AWQ: Activation-aware weight quantization for llm compression and acceleration. *arXiv preprint arXiv:2306.00978*, 2023.

- Haokun Liu, Derek Tam, Mohammed Muqeeth, Jay Mohta, Tenghao Huang, Mohit Bansal, and Colin A Raffel. Few-shot parameter-efficient fine-tuning is better and cheaper than in-context learning. *Advances in Neural Information Processing Systems*, 35:1950–1965, 2022.
- Xiao Liu, Yanan Zheng, Zhengxiao Du, Ming Ding, Yujie Qian, Zhilin Yang, and Jie Tang. Gpt understands, too. *AI Open*, 2023.
- Ilya Loshchilov and Frank Hutter. Decoupled weight decay regularization. *arXiv preprint arXiv:1711.05101*, 2017.
- Shuming Ma, Hongyu Wang, Lingxiao Ma, Lei Wang, Wenhui Wang, Shaohan Huang, Li Dong, Ruiping Wang, Jilong Xue, and Furu Wei. The era of 1-bit llms: All large language models are in 1.58 bits. *arXiv preprint arXiv:2402.17764*, 2024.
- Stephen Merity, Caiming Xiong, James Bradbury, and Richard Socher. Pointer sentinel mixture models. *arXiv preprint arXiv:1609.07843*, 2016.
- Gunho Park, Baeseong Park, Minsub Kim, Sungjae Lee, Jeonghoon Kim, Beomseok Kwon, Se Jung Kwon, Byeongwook Kim, Youngjoo Lee, and Dongsoo Lee. Lut-gemm: Quantized matrix multiplication based on luts for efficient inference in large-scale generative language models. *arXiv preprint arXiv:2206.09557*, 2022.
- Guanghui Qin and Jason Eisner. Learning how to ask: Querying lms with mixtures of soft prompts. *arXiv preprint arXiv:2104.06599*, 2021.
- Alec Radford, Jeffrey Wu, Rewon Child, David Luan, Dario Amodei, Ilya Sutskever, et al. Language models are unsupervised multitask learners. *OpenAI blog*, 1(8):9, 2019.
- Levent Sagun, Leon Bottou, and Yann LeCun. Eigenvalues of the hessian in deep learning: Singularity and beyond. 2017.
- Levent Sagun, Utku Evci, V. Ugur Guney, Yann Dauphin, and Leon Bottou. Empirical analysis of the hessian of over-parametrized neural networks. 2018.
- Yuzhang Shang, Zhihang Yuan, Qiang Wu, and Zhen Dong. PB-LLM: Partially binarized large language models. *arXiv preprint arXiv:2310.00034*, 2023.
- Hugo Touvron, Louis Martin, Kevin Stone, Peter Albert, Amjad Almahairi, Yasmine Babaei, Nikolay Bashlykov, Soumya Batra, Prajjwal Bhargava, Shruti Bhosale, et al. Llama 2: Open foundation and fine-tuned chat models. *arXiv preprint arXiv:2307.09288*, 2023.
- Hongyu Wang, Shuming Ma, Li Dong, Shaohan Huang, Huaijie Wang, Lingxiao Ma, Fan Yang, Ruiping Wang, Yi Wu, and Furu Wei. BitNet: Scaling 1-bit transformers for large language models. *arXiv preprint arXiv:2310.11453*, 2023.
- Tiannan Wang, Jiamin Chen, Qingrui Jia, Shuai Wang, Ruoyu Fang, Huilin Wang, Zhaowei Gao, Chunzhao Xie, Chuou Xu, Jihong Dai, et al. Weaver: Foundation models for creative writing. *arXiv preprint arXiv:2401.17268*, 2024.
- Tianyu Wu, Shizhu He, Jingping Liu, Siqi Sun, Kang Liu, Qing-Long Han, and Yang Tang. A brief overview of chatgpt: The history, status quo and potential future development. *IEEE/CAA Journal of Automatica Sinica*, 10(5):1122–1136, 2023.
- Guangxuan Xiao, Ji Lin, Mickael Seznec, Hao Wu, Julien Demouth, and Song Han. SmoothQuant: Accurate and efficient post-training quantization for large language models. In *International Conference on Machine Learning*, pages 38087–38099. PMLR, 2023.
- Haoran Xu, Young Jin Kim, Amr Sharaf, and Hany Hassan Awadalla. A paradigm shift in machine translation: Boosting translation performance of large language models. *arXiv preprint arXiv:2309.11674*, 2023.
- Zhewei Yao, Reza Yazdani Aminabadi, Minjia Zhang, Xiaoxia Wu, Conglong Li, and Yuxiong He. Zeroquant: Efficient and affordable post-training quantization for large-scale transformers. *Advances in Neural Information Processing Systems*, 35:27168–27183, 2022.
- Susan Zhang, Stephen Roller, Naman Goyal, Mikel Artetxe, Moya Chen, Shuohui Chen, Christopher Dewan, Mona Diab, Xian Li, Xi Victoria Lin, et al. OPT: Open pre-trained transformer language models. *arXiv preprint arXiv:2205.01068*, 2022.
- Zhonghua Zheng, Lizi Liao, Yang Deng, and Liqiang Nie. Building emotional support chatbots in the era of llms. *arXiv preprint arXiv:2308.11584*, 2023.

### A Optimal learning rate for QAFT

While performing hyperparameter grid search on initial learning rate over the set  $\{10^{-6}, 10^{-5}, 10^{-4}, 10^{-3}\}$ , we discovered that the optimal choices strongly correlated with the model size and the quantization precision, which is supported by Fig 4. For a particular model, we observe that QAFT at higher precision such as int8, int6 and int4 favored low learning rates, whereas QAFT at lower precision such as int3 and int2 preferred high learning rates. For a specific format, larger models in the same model family preferred lower learning rates while smaller models in the model family prefers higher learning rates.

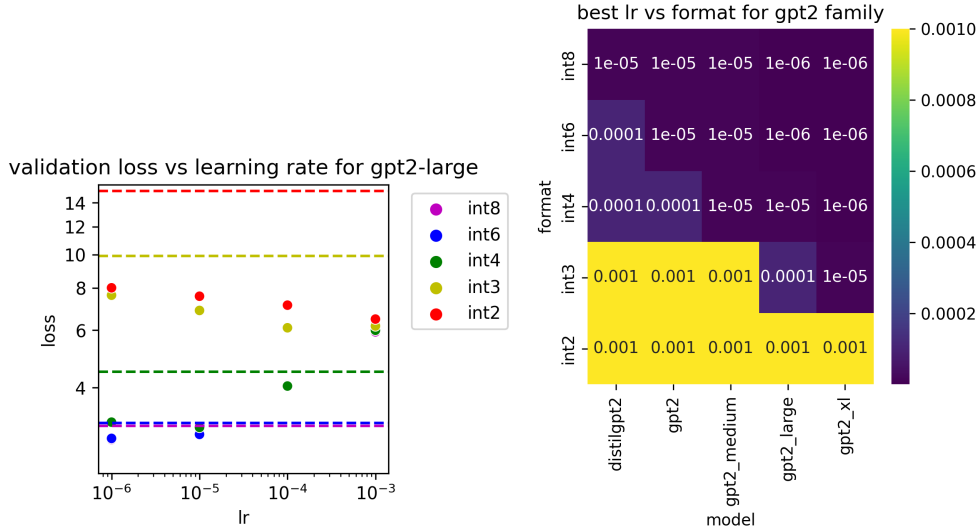


Figure 4: Left: validation NLL loss of gpt2-large after fine-tuning. Dashed lines represent the loss after RTN. Right: best learning rates for GPT-2 family.

### B Effect of number of QAFT iterations

Although we used 8 epochs (1024 iterations) to achieve the most optimal performance, we discovered that QAFT for 1 epoch is sufficient to outperform GPTQ, as shown in Figure 5.

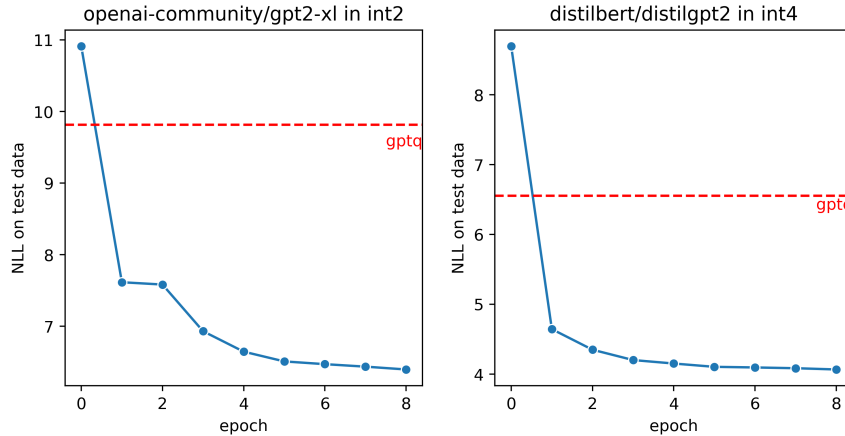
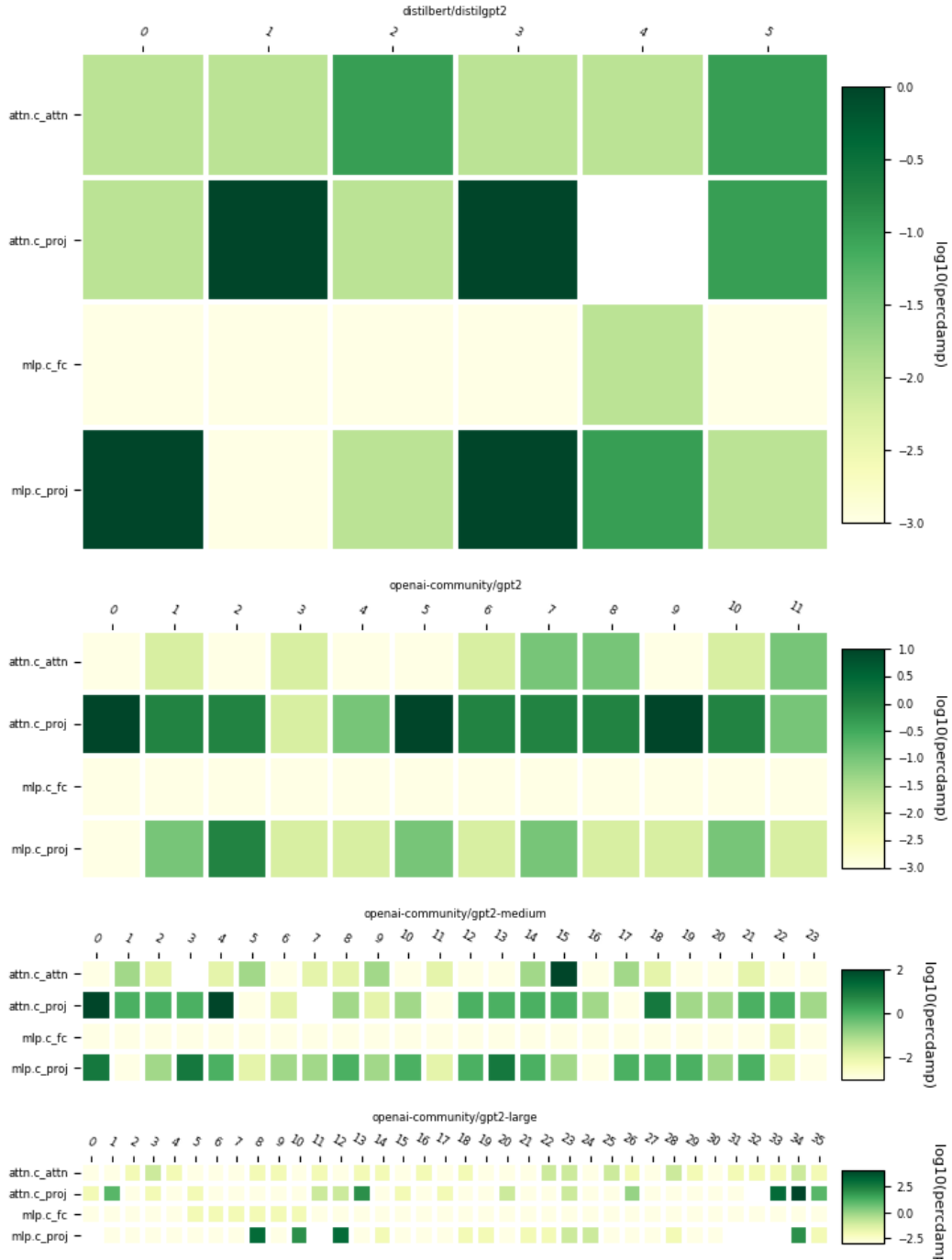


Figure 5: NLL on test data after each epoch of fine-tuning. Epoch 0 represents the NLL of RTN, which is the starting point for fine-tuning. The horizontal red line marks the NLL after GPTQ.

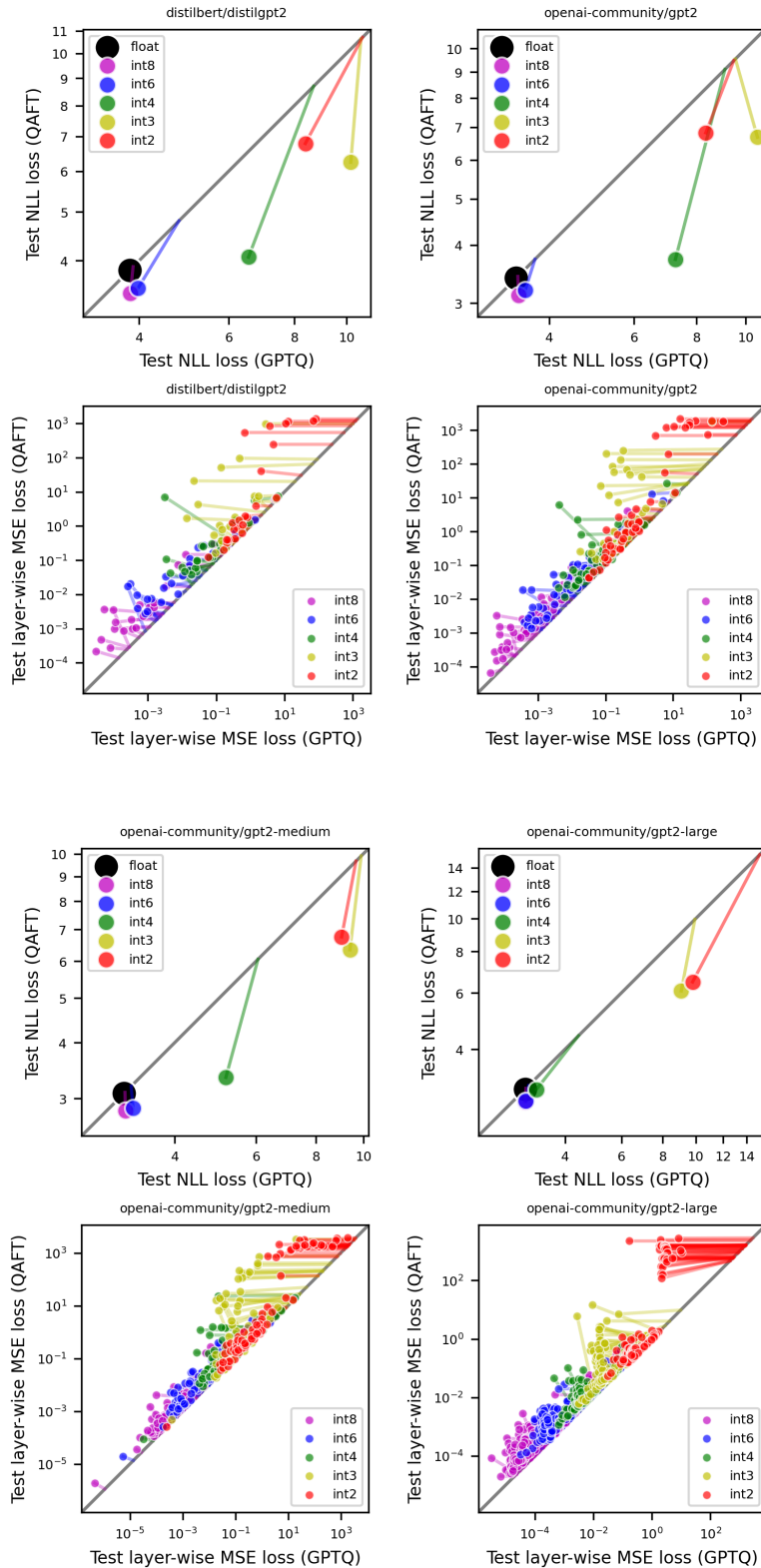
### C Optimal GPTQ dampening factor

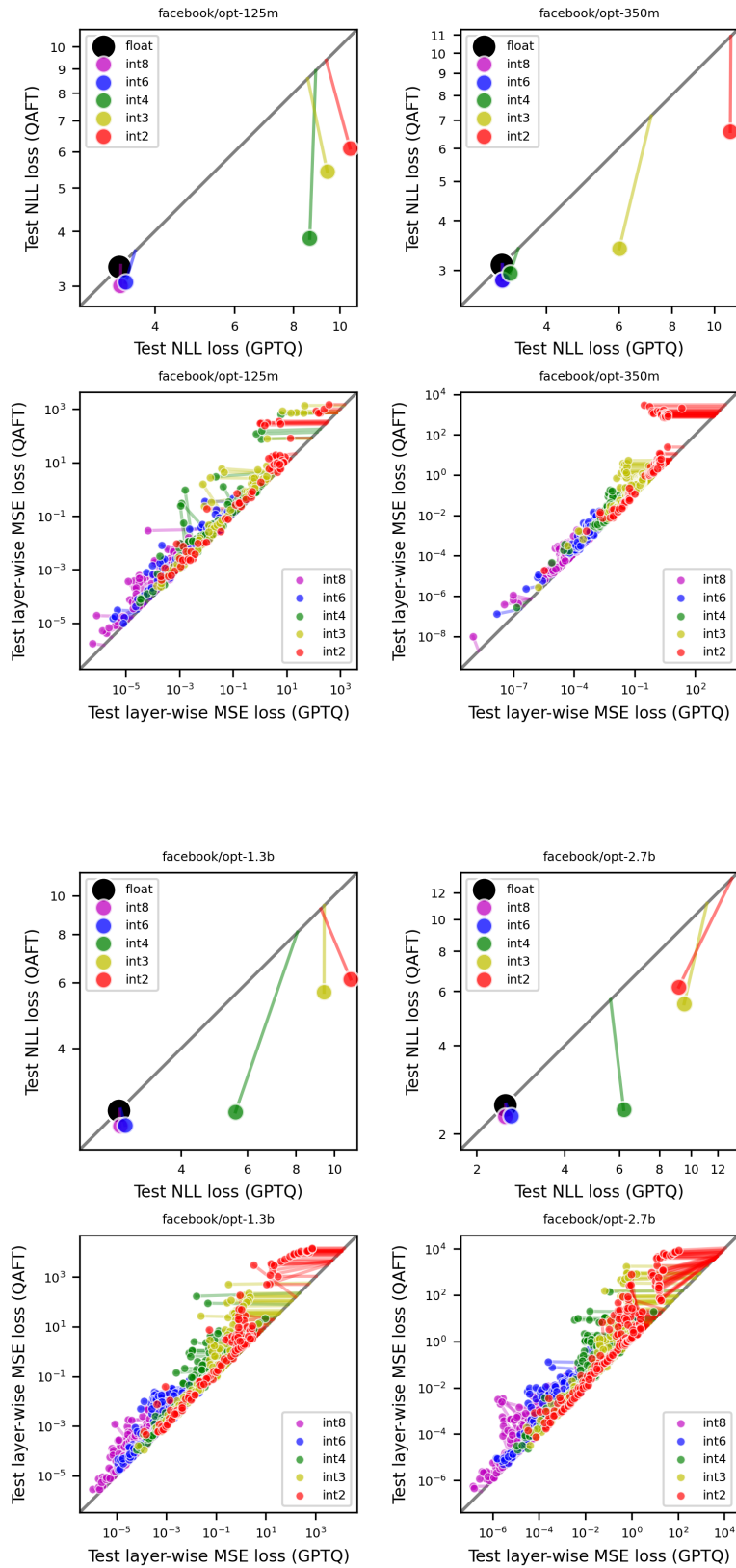
In GPTQ, dampening factor is multiplied with the average diagonal value in Hessian matrix  $H$  and added to the diagonal entries of  $H$  to achieve better numerical stability [Frantar et al., 2022a]. In our experiments, we did a grid search on dampening factor for each layer with the objective of minimizing layer-wise MSE. We visualized the best dampening factor for each quantized layer but failed to find any meaningful patterns.





## D Additional plots for GPTQ vs. QAFT





### E Additional plots for loss landscape

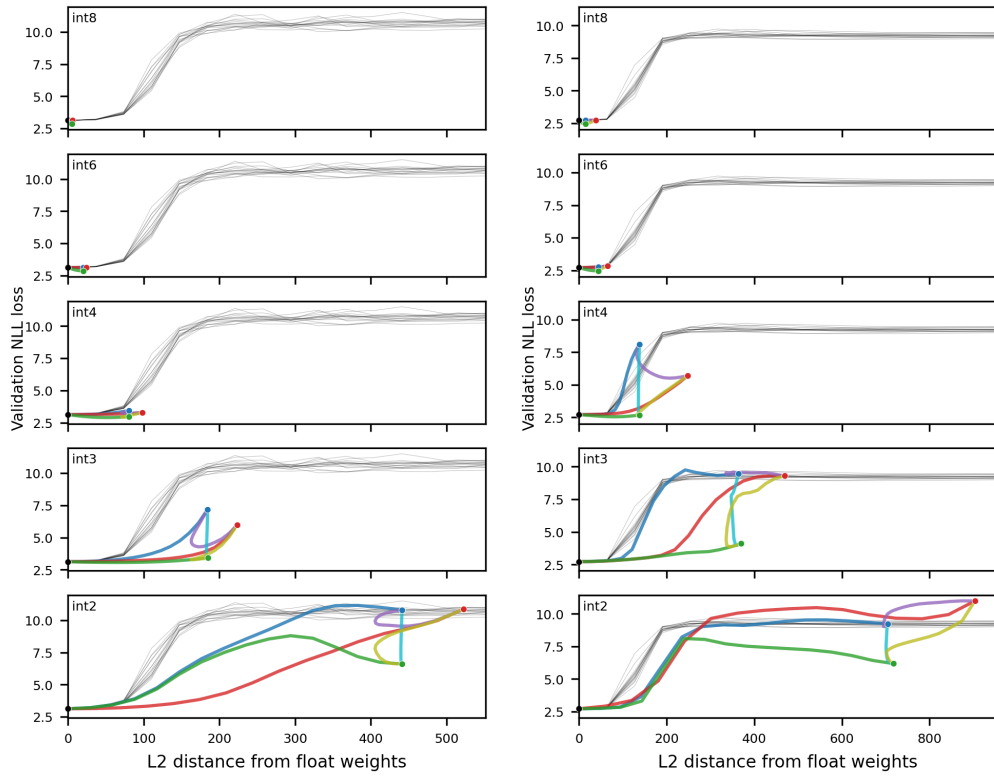


Figure 6: Left: validation loss landscape for opt-350m. Right: validation loss landscape for opt-1.3b. Figure legend consistent with Figure 3.